Journal of Power Sources 187 (2009) 182–189

Contents lists available at ScienceDirect

Journal of Power Sources

journal homepage: www.elsevier.com/locate/jpowsour

Visualisation of water accumulation in the flow channels of PEMFC under various operating conditions

T. Ous*, C. Arcoumanis

Energy and the Environment Research Centre, School of Engineering & Mathematical Sciences, The City University London, United Kingdom

ARTICLE INFO

Article history:
Received 16 June 2008
Received in revised form
18 September 2008
Accepted 19 October 2008
Available online 28 October 2008

Keywords:
PEMFC
Visualisation
Water
Accumulation
Stoichiometry
Flow channels

ABSTRACT

The accumulation of water in the cathode/anode serpentine flow channels of a transparent PEMFC has been investigated by direct visualisation where water droplets and slugs formed in these channels were quantified over a range of operating conditions. Four operating parameters concerning air stoichiometry, hydrogen stoichiometry, cell temperature, and electric load were examined to evaluate their effects on the formation and extraction of water from the flow channels. The results showed that hydrogen and air stoichiometry contribute almost equally to the water formation process in the cathode channels. However, their effects on the water extraction from the channels were quite different. Air stoichiometry proved capable of extracting all the water from the cathode channels, without causing membrane dehydration, contrary to hydrogen. Increasing the operating temperature of the cell was found to be very effective for the water extraction process; a temperature of 60 °C was sufficient to evaporate all the water in the channels as well as enhancing the fuel cell current. The electric load was strongly associated to the water formation in the channels but had no influence on water extraction. Finally, no water was present in the anode flow channels under all examined operating conditions.

1. Introduction

Since the performance of Proton Exchange Membrane Fuel Cells (PEMFC) is strongly dependent on the water distribution and its transport within the cell [1,2], effective water management is essential. To manage the water successfully during PEMFC operation, a number of requirements must be fulfilled. First, the water in the polymer membrane layer should be at high concentration levels to ensure maximum proton (ionic) conductivity through the membrane [3,4]. In contrast, the porous layers mating the polymer membrane, e.g. gas diffusion (GDL), catalyst, and micro-porous layers (MPL), should be water-void to allow the access of reactants to the catalyst site for the reaction of the cell [5]. This delicate balance is usually achieved by changing the hydrophobic and hydrophilic properties of those layers [6]. In addition, water flooding must be prevented at the fuel cell flow channels [7]. Despite the properties of the porous layers to satisfy the water management criteria, unless there is a mechanism to remove the liquid water from the surface of the flow channels; water will gradually build-up and block the channels [8]. The performance of fuel cells is significantly affected by the presence of water in the flow channels [9,10]. As illustrated in Fig. 1, when the channel is completely blocked, the reactants will be forced to bypass through the GDL either into the same channel path or cross over to the adjacent channels depending on the permeability and thickness of the GDL [11]. Although this convective bypass may encourage better water management by driving out more water from the GDL, it prevents the use of the complete catalyst region [12]. Another challenging issue in the water management of PEMFC stems from the distribution of water within the cell. Because of the heterogeneous structure in some of the cell porous layers, achieving a uniform water distribution in the cell is extremely difficult. Uneven water distribution can vary the reactants concentration in different parts of the cell [13] and may cause disturbances to the current flow inside the cell.

Several experimental [14–19] and numerical [20–25] studies have considered various techniques to improve the water management in PEMFC. Some of those techniques were based on optimising the design of fuel cells, e.g. reactant flow channels [18,19,24], Gas Diffusion Layers (GDL) [21], micro-porous layers (MPL) [16,17], and water-removal designs [14,15] while others concentrated on the operating conditions of the cell [20]. The design procedures suggested in [18,19] for the flow channels aimed to enhance the extraction process of water from the channels by the reactants stream. The design in [18] was based on creating an appropriate pressure drop along the channel so that all the liquid water in the cell can be carried away. On the other hand, the emphasis in [19]

* Corresponding author at: SEMS, City University London, Northampton Square, London, EC1V 0HB, United Kingdom. Tel.: +44 7862721125; fax: +44 207 040 8568.
E-mail address: t.ous@city.ac.uk (T. Ous).

0378-7753/$ – see front matter © 2008 Elsevier B.V. All rights reserved.
doi:10.1016/j.jpowsour.2008.10.072

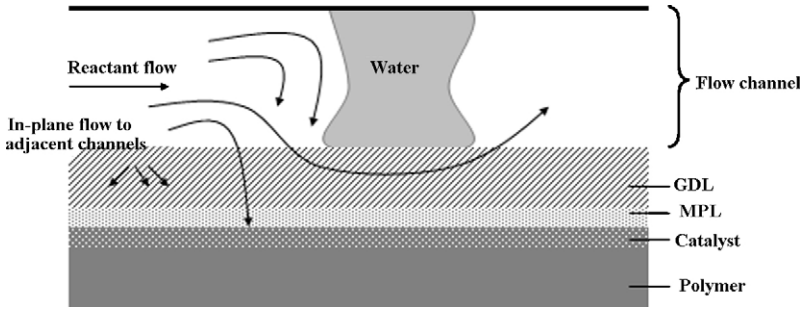

Fig. 1. Reactant flow passage during water blockage in the flow channels.

is on the necessity of matching the design flow field path with the streamline pattern to prevent water flooding in the channels. The role of micro-porous layers (MPL) in improving the water transport and fuel cell performance was highlighted in [16,17]. It was found in [16] that the application of MPLs becomes very important if the carbon paper is prone to flooding, and that MPL could stabilise the current density of the cell under non-humidified reactants flow conditions. Similar results obtained in [17] showed that, although using MPL at the cathode does not affect the water drag coefficient, it improves significantly the fuel cell performance and durability. Different techniques for removing the liquid water from the active reaction sites within the fuel cells, such as vibro-acoustic methods [14] and planar electroosmotic (EO) pumping [15] have been suggested.

Direct visualisation into the cathode flow channels of a transparent PEMFC was carried out in a number of studies [6,8–10] to understand the water accumulation mechanisms as well as the effect of flooding into the performance of the cell during cell reaction. The study in [8] concentrated on the formation of water droplets on the surface of GDL before flooding in the channels takes place. The images showed that flooding is caused by the overlapping of two land-touching droplets developing on each side of the channel. In [10] visualisation was used to monitor simultaneously the effect of water build-up in the channels on the cell current, whereas in [6] and [9] the influence of air stoichiometry and gas diffusion layer on the water-removal process from the channels was investigated, respectively. However, none of these studies has examined the effect of each of the operating conditions of the cell on the water accumulation and its quantity in the flow channels.

In the present study, the effect of the operating conditions on the accumulation of liquid water in PEMFC flow channels has been investigated experimentally through direct visualisation of both anode and cathode channels in order to estimate the amount of water produced by the reaction of the cell. The amount of water observed through the visualisation window has quantified as a function of air stoichiometry, hydrogen stoichiometry, cell temperature, and electric load. These measurements can identify which operating parameters are the most influential on the water formation and extraction from the channels. The cell voltage and current density have been also monitored during the gradual occupation of water in the channels.

2. Experimental

2.1. PEMFC design

The design of the cell used in the present tests is illustrated in Fig. 2. It is based on a single Membrane Electrode Assembly (MEA) from Johnson Matthey (Pt loading 3.5 mg m^{-3}, active area 25 cm^2) sandwiched between two Toray carbon papers (TGP-H-060). The flow channels of both the anode and cathode graphite plates were machined in serpentine shapes with a channel width of 1.5 mm, a depth of 1.5 mm, and a length of 655 mm. Machining was made to one of the flow plates through its entire thickness to allow optical accessibility into the membrane surface underneath. On the top, a transparent end-plate made of Plexiglass was mounted to facilitate direct visualisation into the flow channels. On the other side of the cell, a copper heating plate was incorporated into the design to control the operating temperature of the cell.

2.2. System set-up

Fig. 3 shows a diagram of the experimental set-up which consists of a transparent fuel cell, gas supply units (for hydrogen and air), mass flow controllers, pressure readers, a condenser for water collection, humidity control unit and sensors, a temperature control unit, a CCD camera for image recording, a data acquisition system, and two workstations for operation control and image processing. The air and hydrogen flow rates were regulated using two mass flow controllers, JonCons (0.2–5 L m^{-1}) for air and CT Platon (0.05–0.75 L m^{-1}) for hydrogen. At the inlet and outlet of the cell flow channels, pressure gauges (Stiko) were used to measure the pressure drop across the cell. The water contained in the outlet air stream was collected using a Clarke water separator. The air was humidified using an atomiser (Norgren LO7-200-MPQG) and it was detected together with the temperature by k-type sensors (Honeywell HIH-3610 and HEL-700 series) via an IO data acquisition card (National Instrument PCI-6225) incorporated into workstation 1. Measurements of cell polarization were carried out using the Kelvin connection method which is based on connecting the fuel cell to a variable load (resistors) while another connection from the cell is used for voltage measurements. Both voltage and cur-

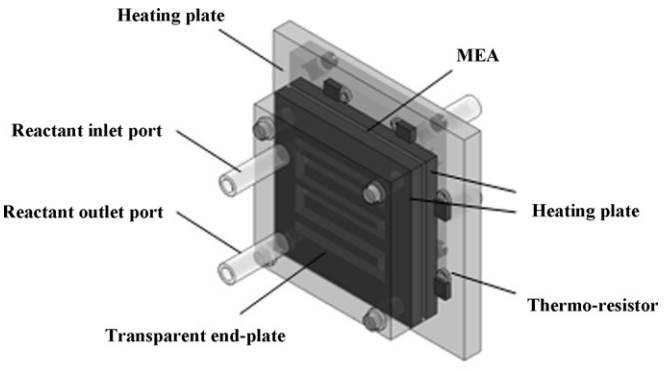

Fig. 2. Transparent PEMFC design.

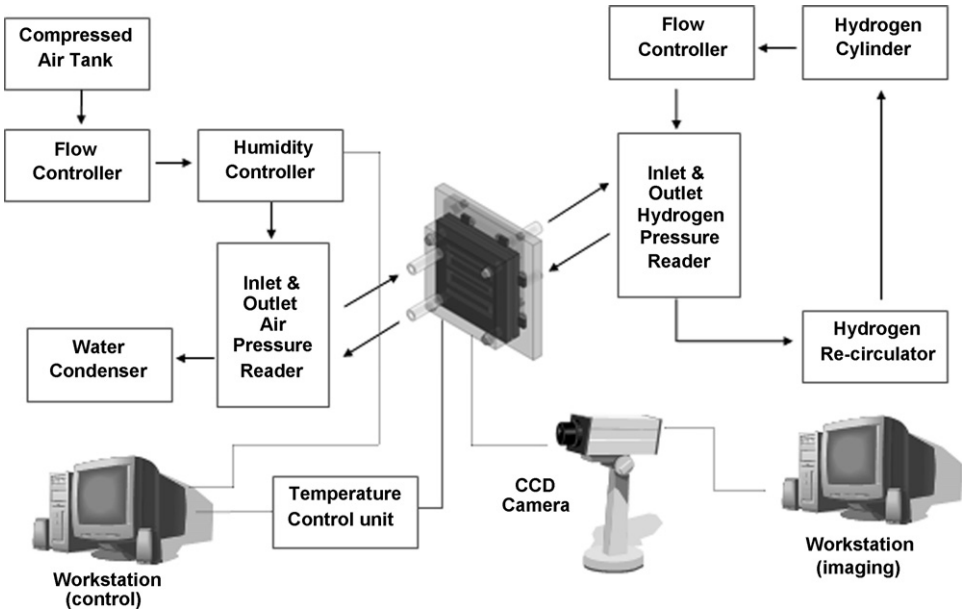

Fig. 3. Schematic of the experimental set-up.

rent values were recorded by the data acquisition system and were displayed by LabView in workstation 1. The operating temperature of the fuel cell was controlled using a built-in temperature controller unit that allows rapid increase of temperature within the range 20–130 °C. The accumulation of liquid water in the cell flow channels was observed using a CCD camera (Sensi-Cam) with adequate delay time of around 2 ms. The obtained images were then transferred into workstation 2 for further processing.

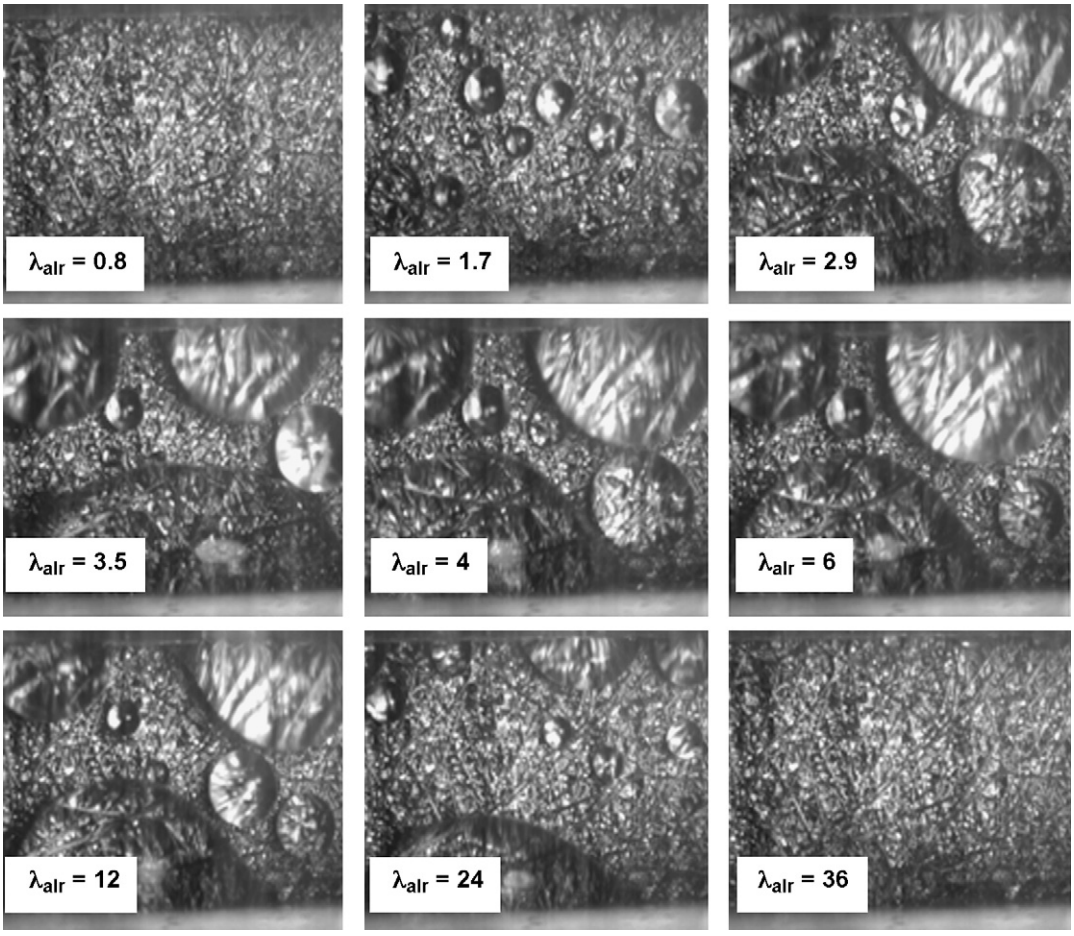

Fig. 4. Images of water accumulation in the cathode flow channels within a range of operating air stoichiometry.

Table 1
Test operating conditions.

Reference operating conditions	Air stoichiometry	Hydrogen stoichiometry	Cell temperature (°C)	Electric load (Ω)	Air inlet humidity RH (%)	Reactant inlet pressure (PSI)
	4	2.8	30	0.1	70	2
Exp. no						
Exp. 1	Varied	2.8	30	0.1	70	2
Exp. 2	4	Varied	30	0.1	70	2
Exp. 3	4	2.8	Varied	0.1	70	2
Exp. 4	4	2.8	30	Varied	70	2

2.3. Water content measurements

Due to the optical arrangement of the camera which allows visualisation of the water droplets only through the top view of the channels, measurement of the droplets volume on the surface is not possible. The images can only give information about the droplets diameter but not the droplets height; this can be overcome by using two cameras, one on the side-wall and the other from the top, to measure droplets in all three dimensions. However, knowing the surface properties of the GDL together with the droplet diameter could be sufficient to estimate the droplet volume. According to Young's equation, interfacial tensions occurring when a droplet brought into contact with a solid surface determine the droplet's contact angle with that surface. The contact angle value can then be used with the droplet diameter to calculate the droplet volume [26]. These calculations become difficult if water appears in the channels in the form of films or slugs instead of droplets. In this experimental work, an additional ex situ test was carried out to study the static behaviour of different droplet sizes on the surface of the GDL (TGP-H-060). These measurements showed that for an average droplet size, around two-thirds of the droplet sphere appear above the surface. This ratio allows droplet volume and height to be calculated from the observed droplet diameter. Since the aim here is just to compare the effect of the operating parameters on the water accumulation in the channels, this measured ratio was assumed for all droplets on the surface; water films were also approximated to match a certain droplet size.

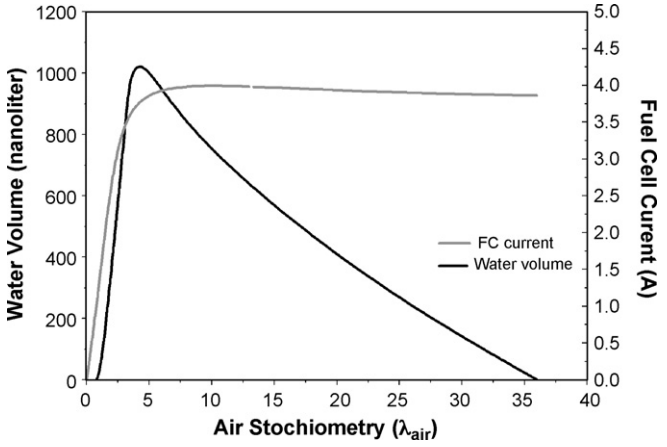

Fig. 5. Effect of air stoichiometry on fuel cell current and water accumulation in the cathode flow channels.

2.4. Operating conditions

Four experiments were carried out to examine the influence of air stoichiometry, hydrogen stoichiometry, temperature, and electric load on the water formation in the flow channels. In each of these experiments, one operating parameter was varied to analyse and compare its effect relative to the other tested parameters. Table 1 lists all operating conditions used. Between each test, the

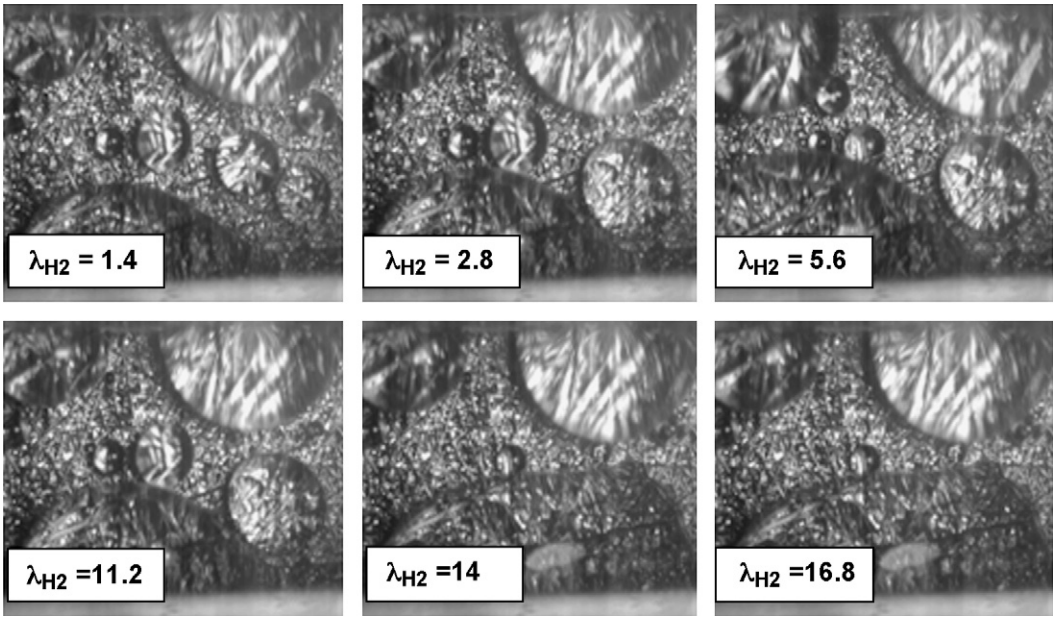

Fig. 6. Images of water accumulation in the cathode flow channels under various operating hydrogen stoichiometry.

fuel cell was dried from water produced by the reaction of the cell to ensure similar initial conditions. The humidity of the air was kept constant at 70% relative humidity for all experiments, whereas hydrogen was dry. Measurements of cell current and voltage were obtained once the cell reached a steady-state condition. The air and hydrogen stoichiometry were calculated at a current density of 200 mA cm^{-2}. Finally, all observations were made into the middle flow channels with an optical size window of 1 mm × 2.8 mm.

3. Results and discussion

3.1. Effect of air stoichiometry

Fig. 4 shows images of water accumulation in the cathode flow channels within a range of air stoichiometry. The images were captured after 10 min from the start of fuel cell operation. It can be seen from Fig. 4 that water droplets of different sizes are formed on the surface and at random locations within the channels. More information about the droplet formation process and the detachment mechanisms can be found in [8].

At an air stoichiometry (λ_{air}) of 0.8, no droplet was observed in the flow channels. As λ_{air} reaches a value of 1.7, droplets start to appear in the channels with an average diameter of around 160 μm. Those droplet sizes were much larger when the air stoichiometry was in the range of 2.9–12 where droplets were mainly generated on the side wall of the channels. When λ_{air} equals 24, droplets were formed in the channels with a wide range of sizes, and were totally removed from the surface by the excessive air flow at λ_{air} = 36. These results are presented quantitatively in Fig. 5, which indicates that the water volume, within the observation area, increases exponentially with air stoichiometry (λ_{air}). As the value of λ_{air} reaches 4, the water quantity starts to drop gradually. It is plausible to stipulate that an increase in the reactant air increases the amount of water produced by the reaction of fuel cells. This is probably valid for small stoichiometry values since air will be consumed only by the reaction. But when the supply of air becomes excessive, the air flow acts rather in a water mass transport role. Switching between these two water phases, rapid production and extraction phase, occurs as illustrated in Fig. 5 once the air stoichiometry reaches a saturation value (e.g. $\lambda_{air\text{-}critical}$ = 4.5). This value is expected to vary from one cell design to another depending on the operating conditions and the design of the fuel cell flow channels.

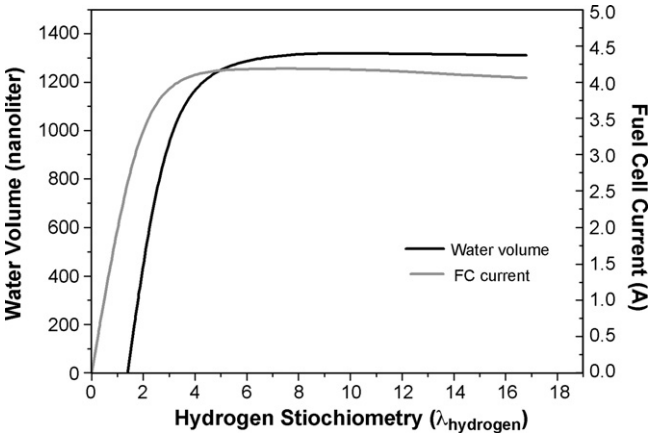

Fig. 7. Effect of operating temperature on fuel cell current and water accumulation in the cathode flow channels.

Fig. 5 also shows the change in fuel cell current during the water production and extraction phases. In the low air stoichiometry range, the current tends to follow a similar trend to the water volume curve. This is because both water and current are directly proportional to the amount of reactant air entering the cell [27]. The current then stabilises as it reaches the air stoichiometry saturation value ($\lambda_{air\text{-}critical}$ = 4.5), and slightly declines at higher air flow indicating the start of membrane dehydration.

3.2. Effect of hydrogen stoichiometry

The effect of hydrogen stoichiometry on the accumulation of water in the cathode flow channels is presented in Figs. 6 and 7. Fig. 6 shows that droplets are formed in the channels, at lower hydrogen stoichiometry (1.4–11.2) and in different sizes, and that at higher λ_{H_2} (>14) droplets tend to be attached to the side wall of the channels. The results of this test are in agreement at low

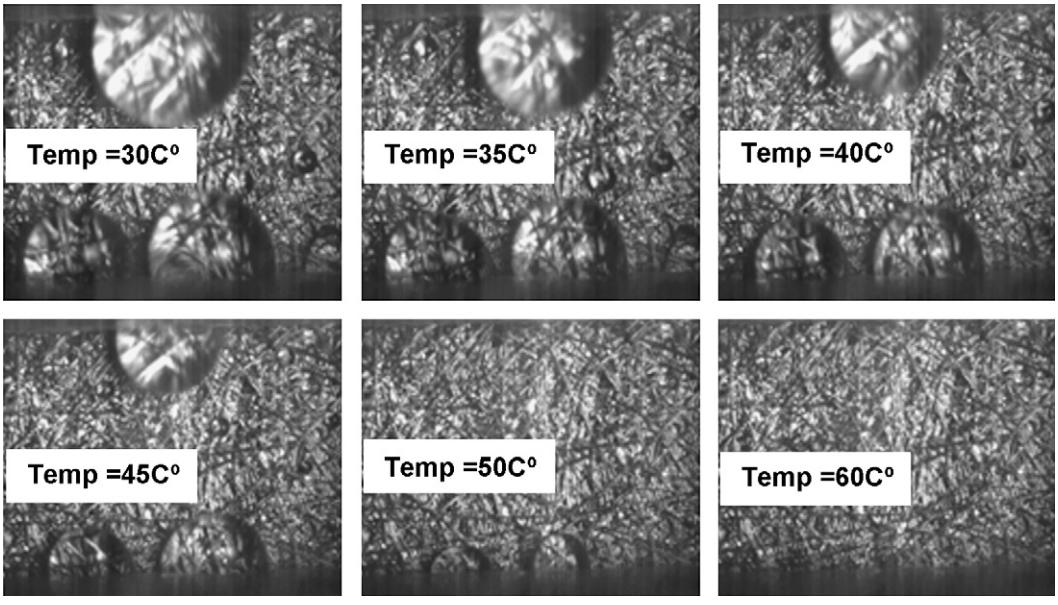

Fig. 8. Images of water accumulation in the cathode flow channels for different fuel cell operating temperatures.

stoichiometry values with those obtained from the air stoichiometry test, both showing an exponential increase of water volume with increasing flow stoichiometry. However, they exhibit differences at the high stoichiometry range. As shown in Fig. 7, when hydrogen stoichiometry exceeds the value of 5.6 the drop in water volume becomes negligible. This implies that hydrogen stoichiometry has minimal influence on the water extraction from the cathode channels; its influence appears to be rather more noticeable in the water production phase. By comparing the maximum amount of water in Figs. 5 and 7 (hydrogen = 1328 nanoliter, air = 1050 nanoliter), it argued that within the area of observation hydrogen stoichiometry contributes more than air towards the water formation in the channels. This is probably due to the stoichiometry of water formation by electrochemical combustion of hydrogen and oxygen that requires two molecules of hydrogen for only one of oxygen. Fig. 6 also shows that the cell current behaves similarly to the water volume during the water production and extraction phases of hydrogen stoichiometry; at low values increases exponentially and then gradually decreases at the higher stoichiometry operating range. The gradual decrease of both the cell current and water mass is likely to be associated with membrane dehydration caused on the anode side of the cell.

3.3. Effect of temperature

The accumulation of water in the channels was examined under different operating temperatures. The fuel cell was heated using the temperature control unit to operate within the range 30–60 °C. Figs. 8 and 9 show the effect of raising the temperature on the amount of water in the observation area. It can be seen from Fig. 8 that most droplets are formed at the side wall of the channels. As the temperature rises, these wall-attached droplets shrink whereas the non-attached ones seem to completely evaporate from the surface. Fig. 9 indicates that the water volume decreases gradually with increasing temperature until it reaches 60 °C at which point no water is visible. This implies that at 60 °C the rate of evaporating of water droplets in the channels becomes faster than their production rate on the surface. Although the water volume decreases with temperature, the fuel cell current continues to increase. This steady increase in the current (~40 mA), as illustrated in Fig. 9, is the result of the reduction in the internal resistance of the fuel cell components. These two advantages when raising the temperature, water extraction and improving the cell current, lead to the conclusion that the temperature is a critical parameter in the operation of fuel cells.

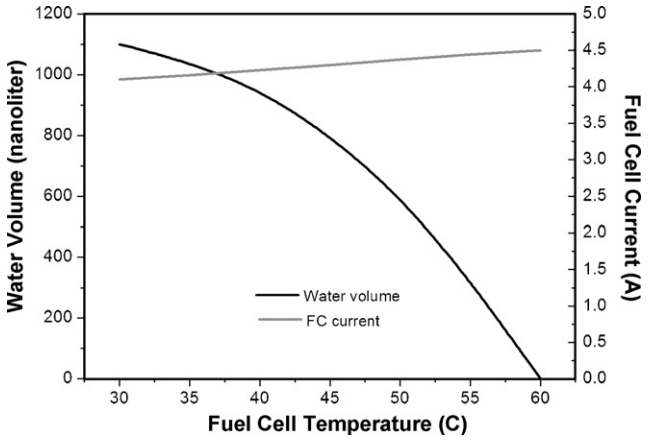

Fig. 9. Effect of operating temperature on fuel cell current and water accumulation in the cathode flow channels.

3.4. Effect of electric load

Fuel cells are expected to draw more current with a minimum electric load connected across their electrodes. However, the more the current generated by the reaction, the more water is expected to appear in the flow channels. This is probably true only if the water-removal mechanisms caused mainly by evaporation and advection are not active during operation. The results presented in Fig. 11 illustrate that water volume in the channels and fuel cell current decline substantially with increasing electric load. When the load reaches 0.5 Ω, the drop in fuel cell current becomes less severe while the water volume continues its sharp drop until it reaches zero at 5.2 Ω. Due to the fact that water and current are the only by-products from the electrochemical reaction of fuel cells, it can be argued that if there is no water in the channels, as in Fig. 10 at 5.2 Ω load, the

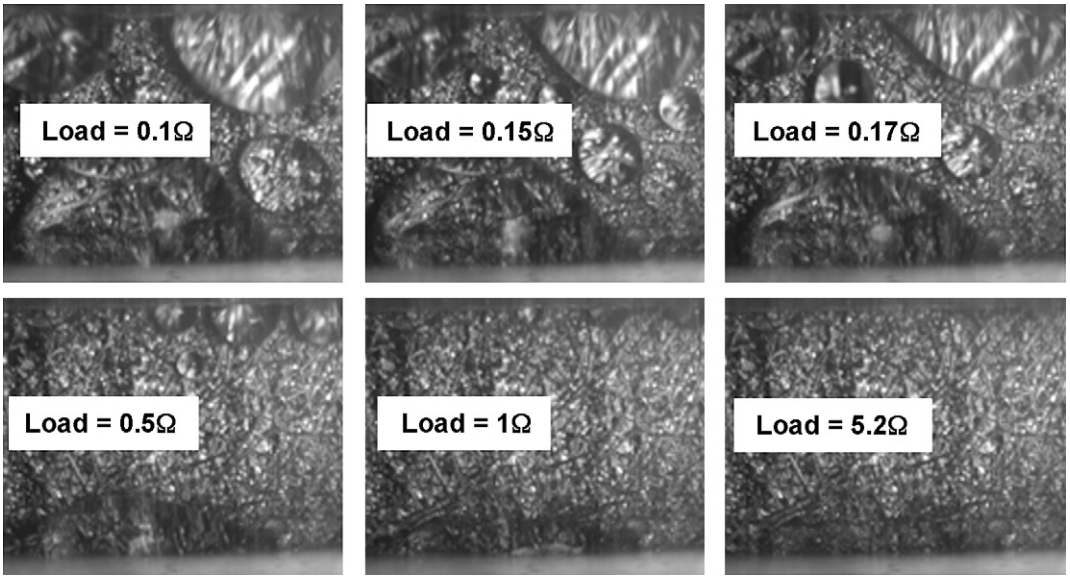

Fig. 10. Images of water accumulation in the cathode flow channels under different electric loads across the fuel cell.

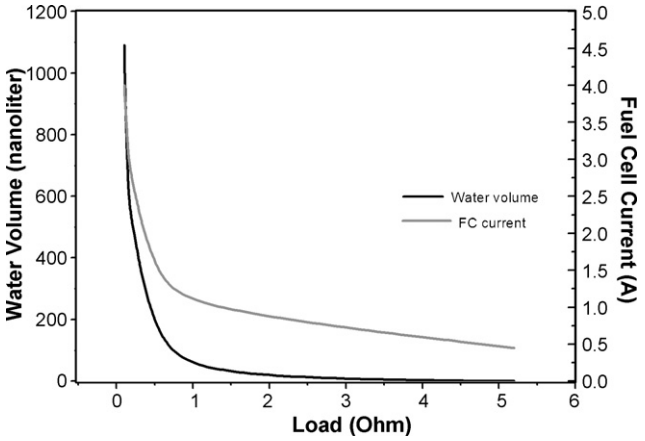

Fig. 11. Effect of electric load on fuel cell current and water accumulation in the cathode flow channels.

cell current will accordingly be zero. However, this is not true since water can still be formed at low production rate at the catalyst and dissipated within the membrane but when it penetrates into the surface of the membrane it is extracted instantly by the air flow before forming any droplets.

3.5. Visualisation at the anode channels

In addition to the observations made of the cathode channels, the anode flow channels were also visualised during fuel cell operation. All the operating conditions mentioned in Table 1 were examined to detect if any water accumulates in those channels. Fig. 12 shows an image in the middle of the anode flow channels under the operating conditions of Exp. 2 listed in Table 1. Even under this extreme water producing condition, no water was observed in the anode flow channels. Probably the amount of water that reaches the anode channels after travelling from the catalyst cathode is so small that the dry hydrogen flow can carry it away before developing on the surface as droplets. Probably these results could be different if the hydrogen entering the channels was humidified.

Fig. 12. Image captured of the anode flow channels under the operating conditions of Exp. 2 in Table 1.

4. Conclusions

The effect of air stoichiometry, hydrogen stoichiometry, temperature, and electric load on the accumulation of water in the anode and cathode flow channels was studied experimentally. Flow visualisation in a transparent PEMFC allowed measurements of the water quantity in the channels. From this analysis, two mechanisms were identified: water formation and water extraction. These mechanisms were influenced differently by each of the examined operating conditions. The air and hydrogen stoichiometry contributed similarly to the water formation at the cathode channels; however, as they reached a saturation value they started extracting water from the channels. The effect of hydrogen during the extraction phase was negligible whereas for the air stoichiometry it was much more noticeable. The increase in temperature was found to be very effective for the water extraction process. Operating the cell at a temperature of 60 °C was sufficient to evaporate all water from the channels. At that point, the evaporation rate was faster than the water formation rate on the surface preventing further formation of water in the channels. Not only it achieved successfully the water extraction from the channels, but the fuel cell current was also enhanced with temperature. This steady increase in the current was the result of a gradual reduction in the bulk and interfacial resistances between the fuel cell components. Furthermore, the effect of electric load was opposite to that of the temperature, having no influence on the water extraction from the channels. Instead, it only determined the amount of water that could be formed based on the amount of current drawn from the cell. Finally, water was not observed in the anode flow channels under all operating conditions.

Acknowledgement

We would like to acknowledge the technical support provided by Johnson Matthey Fuel Cell Group through Dr. Jonathan Sharman and Dr. Jack Frost.

Appendix A. Appendix (Definitions)

Air stoichiometry, λ_{air}, is defined as the ratio of mass flow of air fed into the cell $F_{air\_operating}$ to the mass flow required by the reaction rate at the cathode $F_{air\_required}$. The required mass flow of the reactants $F_{air\_required}$ can be deduced from the total cell current.

Hydrogen stoichiometry, $\lambda_{hydrogen}$, is defined as the ratio of mass flow of hydrogen fed into the cell $F_{hydrogen\_operating}$ to the mass flow required by the reaction rate at the anode $F_{hydrogen\_required}$. The required mass flow of the reactants $F_{hydrogen\_required}$ can be deduced from the total cell current.

References

[1] F. Urbani, O. Barbera, G. Giacoppo, G. Squadrito, E. Passalacqua, Int. J. Hydrogen Energy 33 (2008) 3137–3141.
[2] A. Kraytsberg, Y. Ein-Eli, J. Power Sources 160 (2006) 194–201.
[3] S.-L. Chen, A.B. Bocarsly, J. Benziger, J. Power Sources 152 (2005) 27–33.
[4] Y. Tominaga, I.-C. Hong, S. Asai, M. Sumita, J. Power Sources 171 (2007) 530–534.
[5] S. Litster, G. McLean, J. Power Sources 130 (2004) 61–76.
[6] D. Spernjak, A.K. Prasad, S.G. Advani, J. Power Sources 170 (2007) 334–344.
[7] J.P. Owejan, T.A. Trabold, D.L. Jacobson, M. Arif, S.G. Kandlikar, Int. J. Hydrogen Energy 32 (2007) 4489–4502.
[8] T. Ous, C. Arcoumanis, J. Power Sources 173 (2007) 137–148.
[9] A. Hakenjos, H. Muenter, U. Wittstadt, C. Hebling, J. Power Sources 131 (2004) 213–216.
[10] K. Tüber, D. Pócza, C. Heblin, J. Power Sources 124 (2003) 403–414.
[11] J. Park, X. Li, J. Power Sources 163 (2007) 853–863.

[12] A.A. Shah, G.-S. Kim, W. Gervais, A. Young, K. Promislow, J. Li, S. Ye, J. Power Sources 160 (2006) 1251–1268.
[13] K. Jiao, B. Zhou, P. Quan, J. Power Sources 157 (2006) 226–243.
[14] V. Palan, W.S. Shepard Jr., K.A. Williams, J. Power Sources 161 (2006) 1116–1125.
[15] C.R. Buie, J.D. Posner, T. Fabian, S.-W. Cha, D. Kim, F.B. Prinz, J.K. Eaton, J.G. Santiago, J. Power Sources 161 (2006) 191–202.
[16] Z. Qi, A. Kaufman, J. Power Sources 109 (2002) 38–46.
[17] H.K. Atiyeh, K. Karan, B. Peppley, A. Phoenix, E. Halliop, J. Pharoah, J. Power Sources 170 (2007) 111–121.
[18] X. Li, I. Sabir, J. Park, J. Power Sources 163 (2007) 933–942.
[19] A. Su, F.-B. Weng, C.-Y. Hsu, Y.-M. Chen, Int. J. Hydrogen Energy 31 (2006) 1031–1039.
[20] D. Natarajan, T.V. Nguyen, J. Power Sources 115 (2003) 66–80.
[21] K. Jiao, B. Zhou, J. Power Sources 169 (2007) 296–314.
[22] J.J. Baschuk, X. Li, J. Power Sources 86 (2000) 181–196.
[23] L. Matamoros, D. Brüggemann, J. Power Sources 161 (2006) 203–213.
[24] P. Quan, B. Zhou, A. Sobiesiak, Z. Liu, J. Power Sources 152 (2005) 131–145.
[25] S. Shimpalee, S. Greenway, D. Spuckler, J.W. Van Zee, J. Power Sources 135 (2004) 79–87.
[26] A. Mate, O. Masbernat, C. Gourdon, Chem. Eng. Sci. 55 (2000) 2073–2088.
[27] J. Larminie, A. Dicks, Fuel Cell Systems Explained, second ed., John Wiley & Sons Ltd., 2003.